

Tracing the cosmological assembly of stars and supermassive black holes in galaxies

Andrea Merloni, Gregory Rudnick & Tiziana Di Matteo

Max-Planck-Institut für Astrophysik, Karl-Schwarzschild-Strasse 1, D-85741, Garching, Germany

ABSTRACT

We examine possible phenomenological constraints for the joint evolution of supermassive black holes (SMBH) and their host spheroids. We compare all the available observational data on the redshift evolution of the total stellar mass and star formation rate density in the Universe with the mass and accretion rate density evolution of supermassive black holes, estimated from the hard X-ray selected luminosity function of quasars and active galactic nuclei (AGN) for a given radiative efficiency, ϵ . We assume that the ratio of the stellar mass in spheroids to the black hole mass density evolves as $(1+z)^{-\alpha}$, while the ratio of the stellar mass in disks + irregulars to that in spheroids evolves as $(1+z)^{-\beta}$, and we derive constraints on α , β and ϵ . We find that $\alpha > 0$ at the more than 4-sigma level, implying a larger black hole mass at higher redshift for a given spheroid stellar mass. The favored values for β are typically negative, suggesting that the fraction of stellar mass in spheroids decreases with increasing redshift. This is consistent with recent determinations that show that the mass density at high redshift is dominated by galaxies with irregular morphology. In agreement with earlier work, we constrain ϵ to be between 0.04 and 0.11, depending on the exact value of the local SMBH mass density, but almost independently of α and β .

Key words: black hole physics – galaxies: active – galaxies: evolution – galaxies: nuclei – galaxies: stellar content – quasars: general – cosmology: miscellaneous

1 INTRODUCTION

Recent work has shown that supermassive black holes (SMBH) are ubiquitous in the centers of nearby galaxies. The observational evidence indicates that the mass of the central black hole is correlated with spheroid luminosity and mass (e.g., Kormendy and Richstone 1995; Magorrian et al. 1998) and also with the velocity dispersion of the spheroid (Ferrarese & Merritt 2000; Gebhardt et al. 2000; Tremaine et al. 2002), suggesting that the process that leads to the formation of galactic spheroids must be intimately linked to the growth of the central SMBH. In addition, studies of active galactic nuclei (AGN) hosts in the local universe with the Sloan Digital Sky Survey (SDSS) have also shown that AGN activity is closely related to star formation in local galaxies (Kauffmann et al. 2003; Heckman et al. 2004). From a theoretical perspective, several groups have attempted to investigate the link between the cosmological evolution of QSOs and formation history of galaxies within the context of semi-analytic and numerical models of galaxy formation and evolution (e.g., Monaco et al. 2000; Kauffmann & Haehnelt 2000; Wyithe & Loeb 2003; Di Matteo et al. 2003; Granato et al. 2004; Haiman, Ciotti & Ostriker 2004).

In this paper we make a phenomenological investigation of the link between the growth of black holes and the buildup of their spheroidal hosts over time. Specifically, we compare the evolution of the black hole mass density, ρ_{BH} , to that of the observed mass

density of stars in galaxies, ρ_* , and derive constraints on their co-evolution.

To derive ρ_{BH} as a function of redshift, we use the recently determined mass density of local black holes (Yu & Tremaine 2002; Aller & Richstone 2002; Marconi et al. 2004; Shankar et al. 2004), and evolve it back to $z \sim 3$ using the observed AGN X-ray luminosity functions (see also Merloni 2004 and references therein). The black hole assembly history gathered in such a way assumes that the majority of black hole growth is due to mass accretion and hence is a function of the efficiency associated with mass to (radiative) energy conversion. This provides directly the evolution of mass accretion rate density as well, given by $\dot{\rho}_{\text{BH}} \equiv \Psi_{\text{BH}}$.

To constrain the build-up of stars in the Universe we use the independent measurements of the total star formation rate density (Ψ_*) and the total stellar mass density (ρ_*) evolution. Because current observations indicate that the black hole mass in galaxies is related to the spheroidal component, we will split up the observed ρ_* into two terms. We will hereafter refer to the mass density of stars in spheroids and disks + irregulars as ρ_{sph} and $\rho_{\text{disk+irr}}$ respectively. In addition to counting the mass contribution from pure spheroid, disk, and irregular galaxies, these terms also include masses in the spheroid and disk components of individual galaxies. Estimates of the ratio of $\rho_{\text{disk+irr}}$ to ρ_{sph} at $z = 0$ differ by more than a factor of 5, ranging from 0.2–0.3 (Salucci & Persic 1999; Fukugita, Hogan & Peebles 1998; Fukugita & Peebles 2004) to 1.0–1.2 (Schechter & Dressler 1987; Benson et al. 2002). The redshift evolution of

this ratio should depend not only on the rate of star formation in galaxies of different morphologies at different epochs, but also on the role of mergers, interactions, and secular instabilities in determining galaxy morphology. Both from the theoretical and observational point of view, such an evolution has been so far very hard to quantify (see e.g. Baugh, Cole & Frenk 1996; van den Bosch 1998; Brinchmann & Ellis 2000; Conselice et al. 2004; Combes 2004).

The rest of the paper is organized as follows. In Section 2 we briefly summarize and describe recent measurements of ρ_* and Ψ_* as functions of redshift. In Section 3 we derive the black hole mass density evolution using the X-ray luminosity function and the local black hole mass function. Under the assumption that $\rho_{\text{sph}}(z) \propto \rho_{\text{BH}}(z)(1+z)^{-\alpha}$ and that, at the same time, $\rho_{\text{disk+irr}}/\rho_{\text{sph}}$ evolves as $(1+z)^{-\beta}$, we then compare the history of black hole and total stellar mass assembly in the Universe and derive our global constraints on ϵ , α , and β (Section 4). Finally, in Section 5 we summarize and discuss our results and explore their implications.

Throughout this paper, we adopt a background cosmological model in accordance with the Wilkinson Microwave Anisotropy Probe (*WMAP*) experiment. The model has zero spatial curvature, a cosmological constant, $\Omega_\Lambda = 0.71$ a Hubble constant $H_0 = 72 \text{ km s}^{-1}$, dominated by cold dark matter with $\Omega_m = 0.29$ and $\Omega_b = 0.047$ (Spergel et al. 2003).

2 THE STELLAR MASS DENSITY EVOLUTION

In this work we make use of all available measurements of the stellar mass and star formation rate densities from the literature. The stellar mass density, ρ_* , has been measured in the redshift range from $z = 0$ to $z \sim 3$ from surveys that select galaxies by rest-frame optical or Near Infrared (NIR) light and, in general, estimate the stellar masses and mass-to-light ratios of individual galaxies by fitting spectral synthesis models to optical-NIR spectral energy distributions (see e.g. Brinchmann & Ellis 2000; Cole et al. 2001; Dickinson et al. 2003; Fontana et al. 2003; Drory et al. 2004). One exception is Rudnick et al. (2003) who have determined the evolution in ρ_* from the change in the luminosity density and the global mass-to-light ratio, the latter being determined by using simple models to interpret the cosmically averaged rest-frame optical colors. Although cosmic variance is a dominant source of error for all but the local values, all support a scenario in which ρ_* at $z \sim 3$ was a factor of ~ 7 –20 times lower than it is today and that roughly 50% of the current stellar mass was assembled by $z = 1$ –1.5.

The measurements of ρ_* as a function of redshift also match well with the independently measured integrated global star formation rate density (SFR). The SFR measurements are usually obtained from e.g., optical emission line measurements, MIR dust luminosities, sub-mm observations, or observations of the rest-frame ultraviolet light. These typically show a rapid rise of the SFR(z) out to $z \lesssim 1.5$ where it peaks, followed by a roughly constant level out to at least $z \sim 4$ (see caption of Figure 1 for detailed references).

For the most part, not enough information exists to empirically divide ρ_* and the SFR into different morphological components. However, when comparing these data with ρ_{BH} (see below), it is necessary to take into account the fact that local black hole masses only correlate with the properties of their spheroidal hosts. We account for this by defining a parameter $\lambda(z)$ as the ratio of the mass in disks + irregulars to that in spheroids, in the following way:

$$\rho_*(z) = \rho_{\text{sph}}(z) + \rho_{\text{disk+irr}}(z) = \rho_{\text{sph}}(z)[1 + \lambda(z)]. \quad (1)$$

We then assume that $\lambda(z)$ evolves simply according to $\lambda(z) =$

$\lambda_0(1+z)^{-\beta}$, where λ_0 is the value of the disk to spheroid ratio in the local universe¹.

3 THE BLACK HOLE MASS DENSITY EVOLUTION

Under the standard assumption that black holes grow mainly by accretion, the cosmic evolution of the SMBH accretion rate and its associated mass density can be calculated from the luminosity function of AGN: $\phi(L_{\text{bol}}, z) = dN/dL_{\text{bol}}$, where $L_{\text{bol}} = \epsilon M c^2$ is the bolometric luminosity produced by a SMBH accreting at a rate of \dot{M} with a radiative efficiency ϵ . In practice, the accreting black hole population is always selected through observations in specific wavebands. Crucial is therefore the knowledge of two factors: the completeness of any specific AGN survey, and the bolometric correction needed in order to estimate L_{bol} from the observed luminosity in any specific band.

In recent years, enormous progress has been made in understanding both of the above issues. Here we refer to the discussion of Marconi et al. (2004), who carry out a detailed comparison between optically selected QSOs from the 2dF survey (Boyle et al. 2000), soft X-ray (0.5–2 keV) selected AGN (Miyaji, Hasinger and Schmidt 2000), and hard X-ray (2–10 keV) selected ones (Ueda et al. 2003), and work out the respective bolometric corrections.

The general picture that emerges is that the 2–10 keV AGN luminosity function probes by far the largest fraction of the whole AGN population. This is primarily due to the fact that hard X-rays are less affected by obscuration than either soft X-rays or optical light (Marconi et al. 2004). It has also been shown that most of the obscured sources, which are the major contributor to the X-ray background light, (see e.g. Hasinger 2003, and references therein; Fiore 2003) have typically lower luminosity and lie at a lower redshift than the the optically selected QSOs. Therefore, the growth of SMBH (and of their associated spheroidal hosts) at $z < 1$ is best estimated by studying the evolution of the hard X-ray emitting AGN. At higher redshifts, optical and hard X-ray selection give consistent results (see e.g. Hasinger 2003).

In the following we will indeed assume that the absorption corrected hard X-ray luminosity function of AGN best describes the evolution of the *entire* accreting black holes population between $z = 0$ and $z \sim 3$. For the sake of simplicity, we will adopt for our calculations the luminosity dependent density evolution (LDDE) parameterization of the (intrinsic) 2–10 keV luminosity function described by Ueda et al. (2003).

The redshift evolution of the SMBH accretion rate density can then be easily calculated as follows:

$$\Psi_{\text{BH}}(z) = \int_0^\infty \frac{(1-\epsilon)L_{\text{bol}}(L_X)}{\epsilon c^2} \phi(L_X, z) dL_X, \quad (2)$$

where L_X is the X-ray luminosity in the rest-frame 2–10 keV band, and the bolometric correction function $L_{\text{bol}}(L_X)$ is given by eq. (21) of Marconi et al. (2004), that also takes into account the observed dependence of the optical-to-X-ray ratio α_{ox} on luminosity (Vignali, Brandt & Schneider 2003). This in turn yields for the SMBH mass density:

¹ Since the stellar mass budget at low redshift is overwhelmingly dominated by spheroids and disks, $\rho_{\text{disk+irr}}(z=0) \approx \rho_{\text{disk}}(z=0)$. At high redshift, where irregulars contribute more to the stellar mass density, e.g. Brinchmann & Ellis (2000), $\rho_{\text{disk+irr}} \approx \rho_{\text{disk}} + \rho_{\text{irregular}}$.

$$\frac{\rho_{\text{BH}}(z)}{\rho_{\text{BH},0}} = 1 - \int_0^z \frac{\Psi_{\text{BH}}(z')}{\rho_{\text{BH},0}} \frac{dt}{dz'} dz'. \quad (3)$$

For any given $\phi(L_X, z)$ and bolometric correction, the exact shapes of $\rho_{\text{BH}}(z)$ and Ψ_{BH} then depend only on two numbers: the local black holes mass density $\rho_{\text{BH},0}$ and the (average) radiative efficiency ϵ .

4 THE JOINT EVOLUTION OF THE STELLAR AND BLACK HOLE MASS DENSITIES

Given the derived $\rho_{\text{BH}}(z)$ above, we now want to investigate how the buildup of spheroidal mass in galaxies is related to the buildup of black hole mass over time. We make the simple hypothesis that the redshift evolution of the spheroid and SMBH mass densities are related by the expression:

$$\rho_{\text{sph}}(z) = \mathcal{A}_0 \rho_{\text{BH}}(z) (1+z)^{-\alpha}, \quad (4)$$

where \mathcal{A}_0 is defined by:

$$\mathcal{A}_0 = \rho_{\text{sph},0}/\rho_{\text{BH},0} = \rho_{*,0}/[\rho_{\text{BH},0}(1+\lambda_0)]. \quad (5)$$

For all reasonable values of $\rho_{*,0}$, $\rho_{\text{BH},0}$, and λ_0 , \mathcal{A}_0 is consistent with the expectation from the $M_{\text{BH}} - M_{\text{sph}}$ relation in the local universe (Merritt & Ferrarese 2001; McLure & Dunlop 2002; Marconi & Hunt 2003; Häring & Rix 2004). Then, from eqs. (1) and (4) we obtain the desired relation between total stellar and black hole mass densities:

$$\rho_*(z) = \mathcal{A}_0 \rho_{\text{BH}}(z) (1+z)^{-\alpha} [1 + \lambda_0 (1+z)^{-\beta}]. \quad (6)$$

Finally, the total star formation rate Ψ_* as a function of redshift is given by:

$$d\rho_*(z)/dt = \Psi_*(z) - \int_{z_i}^z \Psi_*(z') \frac{d\chi[\Delta t(z' - z)]}{dt} \frac{dt}{dz'} dz', \quad (7)$$

where $\chi[\Delta t(z' - z)]$ is the fractional mass loss that a simple stellar population experiences after a time Δt (corresponding to the redshift interval $(z' - z)^2$). For simplicity, we fix $z_i = 3.5$, implying that the stellar mass density in place then was formed instantaneously at that redshift. Using the year 2000 version of the stellar population synthesis models of Bruzual & Charlot (1993), we have found a very good approximation for the function χ (for $\Delta t \gtrsim 10^{6.5}$ yr) in the form $d\chi/dt = (\Delta t)^{-1.17}$. With such a prescription, the fractional mass loss after 13 Gyr amounts to about 30%.

We perform a simultaneous fit to the observed stellar mass density and SFR points, assuming the functional forms of (6) and (7) above and calculating the black hole mass density evolution according to eqs. (3) and (2). We vary α , β , and ϵ over the range $[0, 1.5]$, $[-2, 1]$, and $[0.02, 0.3]$ respectively. In Figure 1 we show the observational data for both $\rho_*(z)$ and $\Psi_*(z)$, together with the best fit curves, in this case calculated assuming $\lambda_0 = 0.3$ and $\rho_{\text{BH},0} = 4.2 \times 10^5 M_{\odot} \text{ Mpc}^{-3}$ (Marconi et al. 2004). The shaded areas represent the 1-sigma range of models allowed from the joint fitting of both datasets. It is important to note that, for different possible choices of the local values of $\rho_{\text{BH},0}$ and λ_0 (see below), our best fits for ρ_* and Ψ_* are almost unchanged and always statistically acceptable, with χ^2 values typically ranging from 43 to 45, for

² An analogous term for ρ_{BH} , due to the ejection of SMBHs from galaxy halos after a merger event, is much more difficult to estimate (see e.g. Volonteri, Haardt & Madau 2003) and is neglected here.

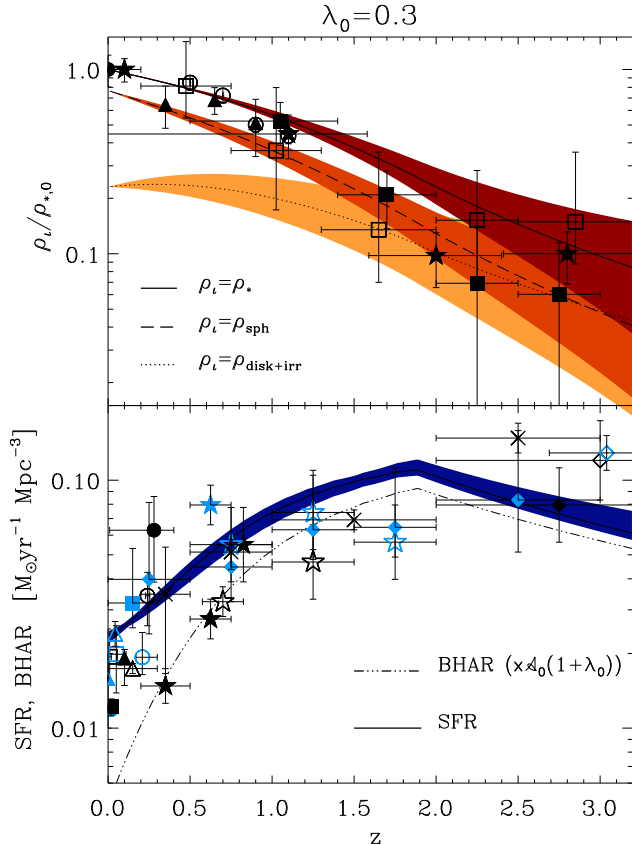


Figure 1. The top panel shows the evolution in the best fit stellar mass density (solid line) as a function of redshift, where the density is given as a ratio to the local value, $\rho_{*,0} = 5.6 \times 10^8 M_{\odot} \text{ Mpc}^{-3}$ (Cole et al. 2001). A value of $\lambda_0 = 0.3$ and $\rho_{\text{BH},0} = 4.2 \times 10^5 M_{\odot} \text{ Mpc}^{-3}$ (Marconi et al. 2004) are adopted here. The darker shaded area represents the 1-sigma confidence interval for ρ_* . Also shown are the relative decomposition of the total stellar mass density into ρ_{sph} (dashed line, grey shaded area) and $\rho_{\text{disk+irr}}$ (dotted line, light grey shaded area), with their corresponding 1-sigma confidence interval. Please note that the absolute normalization - and to a lesser degree the shape - of these two curves depends on the specific value of λ_0 adopted (see text for details). The data points correspond to measurements from the 2dFGRS+2MASS (Cole et al. 2001 – filled circle), the Canada France Redshift Survey (Brinchmann & Ellis 2000 – filled triangles), the MUNICS survey (Drory et al. 2004 – open circles), the Hubble Deep Field North (HDF-N; Dickinson et al. 2003 – filled squares), and the HDF-S (Fontana et al. 2003 – open squares; Rudnick et al. 2003 – filled stars). The lower panel shows the evolution in the best fit SFR (solid line and dark red shaded area) and the corresponding black hole accretion rate density (rescaled by a factor $\mathcal{A}_0(1+\lambda_0)$). The data points correspond to the measurements from Haarsma et al. (2000) – filled black circles; Condon et al. (2002) – filled grey circles; Pascual et al. (2001) – open black circles; Tresse and Maddox (1998) – open grey circles; Gallego et al. (1995), updated following Glazebrook (1999) – filled black squares; Sullivan et al. (2000) – filled grey squares; Serjeant et al. (2002) – open black squares; Glazebrook et al. (2003) – open grey squares; Brinchmann et al. (2004) – filled black triangles; Gallego et al. (1995) – filled grey triangles; Treyer et al. (1998) – open black triangles; Gronwall (1998) – open grey triangles; Lilly et al. (1996) – filled black stars; Flores et al. (1999) – filled grey stars; Cowie et al. (1996) – open black stars; Connolly et al. (1997) – open grey stars; Madau, Pozzetti and Dickinson (1998) – filled black diamonds; Pascale, Lanzetta & Fernandez-Soto (1998) – filled grey diamonds; Hughes et al. (1998) – open black diamonds; Steidel et al. (1999) – open grey diamonds; Sawicki et al. (1997) – black crosses.

55 degrees of freedom. Nonetheless, it is apparent from Fig. 1 that the best fit solution for ρ_* systematically overpredicts the observed points in the redshift range $1.5 \lesssim z \lesssim 2$, where, however, cosmic variance plays a large role and the ρ_* measurements are quite uncertain.

Also shown in Fig. 1 are the relative contributions to the total stellar mass density of ρ_{sph} and $\rho_{\text{disk+irr}}$. It should be stressed that such a decomposition is strongly dependent on λ_0 . The *relative* growth in spheroids and disks + irregulars relative to their respective local values is in fact well represented by these curves, as it mainly depends on the value of β , but their absolute growth, and hence the total mass density in disks + irregulars relative to that in spheroids at any z , is highly dependent on the adopted value of λ_0 . For example, if $\lambda_0 = 1.0$, the dashed and dotted lines in Fig. 1 will be moved vertically to attain the same value at $z = 0$.

In Figure 2 we show the results as probability contours in the 2-D parameter space (ϵ, α) , obtained by marginalizing the total probability distribution over β , assuming a flat prior on its distribution, to be conservative. The results are shown for two possible values of the parameter λ_0 (0.3 and 1). As it is well known, a constraint on the average radiative efficiency of accreting SMBH can be obtained by comparing the total mass of the relic population with the integrated light from all AGN at all redshifts (Soltan 1982; Yu & Tremaine 2002; Marconi et al. 2004). Given a reliable inventory of all the light emitted during the accretion induced growth phase (here assumed to be given by the HXLF of AGN), the final result will depend crucially on the value of the local SMBH mass density: the lower $\rho_{\text{BH},0}$ is, the higher the radiative efficiency has to be in order not to over-produce the locally measured density of relic black holes. This is clearly illustrated by Figure 2, that shows the calculated confidence limits assuming two different priors for $\rho_{\text{BH},0}$. In one case, shown by the rightmost (b) contours, we have adopted a lower value as derived, for example, by Yu & Tremaine (2002) of $\rho_{\text{BH},0} = 2.5 \times 10^5 M_\odot \text{Mpc}^{-3}$. The radiative efficiency is constrained, at the 3-sigma level, between $0.08 \lesssim \epsilon \lesssim 0.11$. On the other hand, if the local SMBH mass density is as high as $\rho_{\text{BH},0} = 4.2 \times 10^5 M_\odot \text{Mpc}^{-3}$, as suggested by Marconi et al. (2004), the radiative efficiency is allowed to take a lower value and is constrained, at the 3-sigma level between $0.05 \lesssim \epsilon \lesssim 0.07$, as shown by the leftmost (a) contours. In fact, the range of allowed radiative efficiencies would have been larger than those shown in Fig. 2 had we also considered the uncertainties on the measures of the local black hole mass density³. It is clear that there is almost complete degeneracy between ϵ and $\rho_{\text{BH},0}$, once the luminosity function of AGN is fixed. Efficiencies lower than 0.04 are excluded at the more than 4-sigma level, whatever the prior on the local SMBH mass density, provided that it is not higher than $6.5 \times 10^5 M_\odot \text{Mpc}^{-3}$. This is easily understood, as black holes accreting with $\epsilon < 0.04$ build up, in the redshift interval between $z = 0$ and $z = 3$, a mass larger than this value.

Figure 3 shows the probability contours in the 2-D parameter space (β, α) , obtained by marginalizing the total probability distribution over ϵ , assuming a flat prior on its distribution, once again calculated for two different values of λ_0 . We note here that the constraints on these two parameters are almost independent of

³ We note here that the main difference between the two values of $\rho_{\text{BH},0}$ comes from a higher normalization of the $M-\sigma$ relation by a factor 1.6 adopted by Marconi et al. (2004). It is beyond the scope of this letter to discuss thoroughly the reason of this discrepancy. The reader is referred to Yu and Tremaine (2002) and to Marconi et al. (2004) for such a discussion.

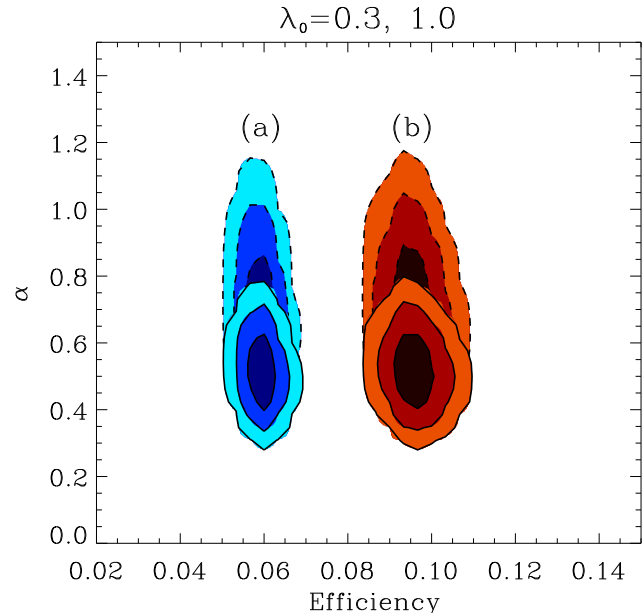


Figure 2. The 1, 2 and 3 sigma confidence levels for the parameters α and ϵ obtained by simultaneously fitting the redshift evolution of the total stellar mass density and of the total star formation rate density with eqns. (6) and (7), respectively, marginalizing over the other parameter, β , assuming a flat prior on its probability distribution between $-2 < \beta < 1$. Four sets of contours are plotted. Solid lines correspond to a local ratio of the disk + irregular to spheroid stellar mass density of $\lambda_0 = 0.3$; dashed to $\lambda_0 = 1.0$. Left (a) contours are for $\rho_{\text{BH},0} = 4.2 \times 10^5 M_\odot \text{Mpc}^{-3}$ (Marconi et al. 2004), while the right (b) ones correspond to $\rho_{\text{BH},0} = 2.5 \times 10^5 M_\odot \text{Mpc}^{-3}$ (Yu and Tremaine 2002).

the adopted value for $\rho_{\text{BH},0}$. The two sets of contours in figure 3 can be understood as follows. At low redshifts, $\Psi_{\text{BH}} \ll 1$, and $\rho_{\text{BH}} \sim \text{const}$. Therefore, from eq. (6), we see that the observed decline of the total stellar mass density, and the corresponding increase of the star formation rate density, will be driven by the term $(1+z)^{-\alpha}[1 + \lambda_0(1+z)^{-\beta}]$. For low values of z , this term can be approximated by $(1+z)^{-\gamma}$, with $\gamma \simeq \alpha + \beta\lambda_0/(1+\lambda_0)$, and fitting the low redshift points (see below) with this simple expression we obtain the relation $\alpha + \beta\lambda_0/(1+\lambda_0) \approx 0.3$, which indeed determines the approximate direction along which the best fit parameters α and β are allowed to move.

As it is expected, the lower the value of λ_0 , the less constrained will the parameter β be. A constant $\lambda(z)$ ($\beta = 0$) is allowed at the 3-sigma level only if $\lambda_0 < 0.3$, but the best fit value always correspond to a negative β , i.e. to an increase of the disk/irregulars stellar mass fraction with respect to the spheroid one with increasing redshift.

To further test the sensitivity of our constraints on α , β and ϵ we have also performed a fit restricted to the redshift interval $0 \leq z \leq 1$, where the observational data points are more numerous and have smaller error bars. In doing this, we have found that while the constraints on α and β remain virtually unchanged, those on the radiative efficiency are much looser. In particular, for high values of the local SMBH mass density, we find that $0.03 \lesssim \epsilon \lesssim 0.12$ at the 3-sigma level. This can be understood because the constraint on ϵ comes primarily from the epoch in which the black hole accretion rate density is highest, which occurs at $z > 1$, where the QSO luminosity function peaks. The data at $z < 1$ don't serve to strongly constrain ϵ .

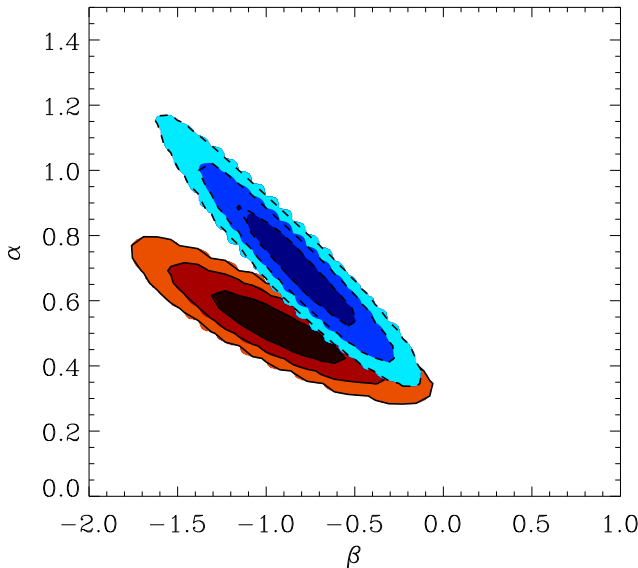


Figure 3. The contours show the 1, 2 and 3 sigma confidence levels for the parameters α and β obtained by simultaneously fitting the redshift evolution of the stellar mass density and of the star formation rate density with eqns. (6) and (7), respectively, and then marginalizing over the radiative efficiency of black holes, ϵ , assuming a flat prior on its probability distribution between $0.02 < \epsilon < 0.4$. Solid contours correspond to the case in which we fix the local ratio of disk + irregular to spheroid stellar mass density to $\lambda_0 = 0.3$, dashed contours correspond to the case of $\lambda_0 = 1$. The two parameters are degenerate along the line $\alpha + \lambda_0\beta/(1 + \lambda_0) \approx 0.3$ (see text for details).

In summary, irrespective of all the uncertainties in the determination of λ_0 and in the high redshift stellar mass and star formation rate points, the data do indeed put some constraints on the redshift evolution of $\rho_{\text{sph}}/\rho_{\text{BH}}$. In particular, a constant ratio, $\alpha = 0$ is excluded at a more than 4-sigma confidence level, implying that the black hole to spheroid mass density ratio must have been larger in the past.

5 DISCUSSION

It is well known that both AGN activity and SFR decline at low redshift. Moreover, the correlation observed locally between supermassive black hole masses and global properties of their host spheroids are suggestive of a fundamental link between the formation and evolution of black holes and galaxies.

In this letter we have attempted to constrain phenomenologically the joint evolution of supermassive black holes, their host spheroids and the total stellar mass density in the universe.

We have assumed that the black hole mass density evolution is due to accretion only and that it can therefore be reliably reconstructed from the local black hole mass density and from the redshift evolution of the hard X-ray luminosity function of AGN/QSO, with the (average) radiative efficiency of accretion, ϵ as the only free parameter. We have then examined the relation between ρ_{BH} and ρ_{sph} , assuming that the ratio of these two densities simply evolves as $(1 + z)^{-\alpha}$. Finally, we have considered the simple case in which the ratio of the stellar mass density in disk components + irregular galaxies to that of the spheroid component of galaxies evolves as $\lambda(z) \propto (1 + z)^{-\beta}$. By fitting simultaneously

all the available observational data on the total stellar mass density and star formation rate density as a function of redshift, we have obtained a set of constraints on the three model parameters $(\epsilon, \alpha, \beta)$, which themselves depend on the local values of ρ_{BH} and λ .

We have shown that the constraint we obtain on the radiative efficiency of accretion crucially depends on the adopted value for the local black hole mass density, but not on α or β .

More importantly, we have shown that BH accretion does not exactly track either the spheroid nor the total star assembly (i.e. both α and $\gamma = \alpha + \lambda_0\beta/(1 + \lambda_0)$ are larger than zero). This is the most important result of our study: irrespective of the exact mass budget in spheroids and disks + irregulars, the ratio of the total or spheroid stellar to black hole mass density was lower at higher redshift. The simultaneous fit we obtain for both ρ_* and Ψ_* also indicates that the black hole growth rate is suppressed with respect to the total SFR at $z < 2$, as it can be seen in Figure 1 (as also shown in the cosmological simulations of Di Matteo et al. 2003).

Our findings have a direct *observable* consequences for the expected redshift evolution of the $M_{\text{BH}} - M_{\text{sph}}$ relationship: $\alpha > 0$ implies a larger black hole mass for a given host spheroid mass at higher redshift.

We can also compare our results with recent semi-analytical work that tries to incorporate SMBH growth and feedback into a galaxy evolution scenario. The simplest way to relate black hole mass and global galactic properties is via an energy argument, as discussed, for example, in Wyithe and Loeb (2003): a SMBH will stop growing as soon as the energy provided by accretion onto it at a fraction η of the Eddington rate for a time t_Q will equal the binding energy of the gas in the DM halo: $M_{\text{BH}}\eta L_{\text{Edd},\odot}t_Q F_Q = \frac{1}{2}\Omega_b\Omega_m M_{\text{halo}}v_c^2$. Here, the black hole mass is in solar units, $L_{\text{Edd},\odot}$ is the Eddington rate of a one solar mass black hole, F_Q is a coupling coefficient that can be determined from the normalization of the $M_{\text{BH}} - \sigma$ relation, Ω_m and Ω_b are the matter and baryon densities, respectively, and $M_{\text{halo}} v_c$ are the mass and circular velocity of a DM halo. Most of the feedback models in the recent literature (Kauffmann and Haenelt 2000; Cavaliere & Vittorini 2002; Menci et al. 2003; Wyithe and Loeb 2003; Granato et al. 2004) assume (sometimes implicitly) a linear proportionality between the quasar lifetime and the dynamical time of the dark matter halo in which it is embedded: $t_Q = t_{\text{dyn}} \propto \xi(z)^{-1/2}(1 + z)^{-3/2}$, where $\xi(z)$ is a weak function of z and depends on the cosmological parameters only (see e.g.; Barkana and Loeb 2001 for more details). Indeed, Wyithe and Loeb (2003) have shown that, if the QSO lifetime is equal to the dynamical time of a DM halo, then the $M_{\text{BH}} - \sigma$ relation does not change with redshift, while the ratio of the black hole to (spheroid) stellar mass density should evolve as $\rho_{\text{sph}}/\rho_{\text{BH}} \propto [\xi(z)]^{-1/2}(1 + z)^{-3/2} \sim (1 + z)^{-1.15}$, where the final approximation is valid for $0 < z < 2$. Comparing this with the constraints on α we have obtained in section 4, we see that, although marginally consistent with these simple semi-analytical schemes, and only for the high λ_0 case, the data clearly suggest a slower evolution for the spheroid to black hole mass ratio than that predicted by just assuming a constant $M_{\text{BH}} - \sigma$ relation at all z . Therefore, this would imply that the normalization of the $M_{\text{BH}} - \sigma$ relation *should evolve* with redshift. A caveat is however in place here, as of course η and F_Q in prescriptions such as those of Wyithe and Loeb (2003) may not be constant, but vary as a function of black hole mass, or mass accretion and as function of redshift (e.g.; Merloni 2004). Observational tests of the $M_{\text{BH}} - \sigma$ and $M_{\text{BH}} - M_{\text{sph}}$ relations at higher redshift (see e.g. Shields et al. 2003) will be crucial to our understanding of the interplay between black holes and their host galaxies.

6 Merloni, Rudnick & Di Matteo

Finally, our results suggest that the fraction of ρ_* locked up into the non-spheroidal components of galaxies and in irregular galaxies should increase with increasing redshift. This result is consistent with Brinchmann & Ellis (2001) that show that the mass density in irregulars increases rapidly out to $z \sim 1$.

If we relax the assumption that black hole mass and spheroid mass densities are related at all redshifts, then ρ_{sph} and $\rho_{\text{disk+irr}}$ in eq. (1) would simple correspond to the stellar mass that *ends up* in spheroids and disks, respectively, at $z = 0$, where we know that black hole mass and spheroid mass are related. Under this assumption, negative values of β would imply that the stars in local spheroids were formed at a later time than the stars in present day disks. This would directly contradict the relative observed ages of disks and spheroids. On the other hand, no such contradiction occurs when using our adopted assumption, i.e. that there is a $M_{\text{BH}} - M_{\text{sph}}$ relation at all redshifts and that ρ_{sph} and $\rho_{\text{disk+irr}}$ correspond, at any given redshift, to the mass in spheroids and disks + irregulars respectively. This further supports the idea that the dynamical events that lead to the assembly of spheroid stellar mass (mergers, secular instabilities, gas accretion, etc.) are directly linked to the major accretion events onto the SMBH.

The upcoming results from projects such as the GEMS (Galaxy Evolution from Morphological Studies; see Rix et al. 2004) survey, that will provide morphologies and structural parameters for nearly 10,000 galaxies at $0.2 \lesssim z \lesssim 1.1$ and their respective contributions to the mass density, will surely improve our understanding of this issue, and will possibly help us to better understand how the simultaneous evolution of black holes, spheroids, and disks in galaxies proceeded.

ACKNOWLEDGMENTS

We thank J. Brinchmann, A. Fontana, and V. Springel for providing us with some of the observational data on star formation and stellar mass density. G.R. acknowledges the support by the Deutsche Forschungsgemeinschaft (DFG), SFB 375 (Astroteilchenphysik).

REFERENCES

Aller M. C. & Richstone D., 2002, AJ, 124, 3035
 Barkana R., Loeb A., 2001, Phys. Rep., 349, 125
 Baugh C. M., Cole S. & Frenk C. S., 1996, MNRAS, 283, 1361
 Benson A. J., Frenk C. S., Sharples R. M., 2002, ApJ, 574, 104
 Boyle B. J., Shanks T., Croom S. M., Smith R. J., Miller L., Loaring N., Heymans C., 2000, MNRAS, 317, 1014
 Brinchmann J., Ellis R. S., 2000, ApJL, 536, L77
 Brinchmann, J., Charlot S., White S. D. M., Tremonti C., Kauffmann G., Heckman T., Brinkmann J., 2004, MNRAS, 351, 1151
 Bruzual G. & Charlot S., 1993, ApJ, 405, 538.
 Cattaneo A. & Bernardi M., 2003, MNRAS, 344, 45
 Cavaliere A. & Vittorini V., 2002, ApJ, 570, 114
 Cole S. et al., 2001, MNRAS, 326, 255
 Combes F., 2004, in "Penetrating Bars through Masks of Cosmic Dust: the Hubble Tuning Fork Strikes a New Note", Pilanesberg, ed. D. Block et al., Kluwer, in press. astro-ph/0406306
 Condon J. J., Cotton W. D., Broderick J. J., 2002, AJ, 124, 675
 Connolly A. J., Szalay A. S., Dickinson M. E., SubbaRao M. U., Brunner R. J. 1997, ApJL, 486, L11
 Conselice C., et al. 2004, ApJL, 600, L139
 Cowie L. L.; Songaila A.; Hu E. M., Cohen J. G., 1996, AJ, 112, 839
 Di Matteo T., Croft R. A. C., Springel V. & Hernquist L., 2003, ApJ, 593, 56
 Dickinson M., Popovich C., Ferguson H., Budavári T., 2003, ApJ, 587, 25
 Drory N., Bender R., Feulner G., Hopp U., Maraston C., Snigula J., Hill G. J., 2004, ApJ, 608, 742
 Fabian A. C., 2003, to appear in "Coevolution of Black Holes and Galaxies", Carnegie Observatories Astrophysics Series, Vol. 1: ed. L. Ho (Cambridge: CUP). astro-ph/0304122
 Ferrarese, L. & Merritt, D., 2000, ApJL, 539, L9
 Fiore F. et al., 2003, A&A, 409, 79
 Flores H. et al., 1999, ApJ, 517, 148
 Fontana et al., 2003, ApJL, 594, L9
 Fukugita M., Hogan C. J., Peebles, P. J. E., 1998, ApJ, 503, 518
 Fukugita M., Peebles, P. J. E., 2004. astro-ph/0406095
 Gallego J., Zamorano J., Aragón-Salamanca A., Rego M., 1995, ApJL, 455, L1
 Gebhardt, K. et al., 2000, ApJL, 539, L13
 Glazebrook K., Blake C., Economou F., Lilly S., Colless M., 1999, MNRAS, 306, 843
 Glazebrook K. et al., 2003, ApJ, 587, 55
 Granato G.L., De Zotti G., Silva L., Bressan A. & Danese L., 2004, ApJ, 600, 580
 Gronwall C., in The Young Universe, Eds. S. D'Odorico, A. Fontana, and E. Giallongo. ASP Conference Series; Vol. 146; 1998, p.96
 Haarsma D. B., Partridge R. B., Windhorst R. A., Richards, E. A., 2000, ApJ, 544, 641
 Haiman Z. & Loeb A., 1998, ApJ, 503, 505
 Haiman Z., Ciotti L., Ostriker J. P., 2004, ApJ, 606, 763
 Häring N., Rix H.-W., 2004, ApJL, 604, L89
 Hasinger G., 2003, AIP Conf. Proc. 666 (2003) 227-236
 Heckman T. M., Kauffmann G., Brinchmann J., Charlot S., Tremonti C. & White S., 2004, ApJ, in press. astro-ph/0406218
 Hernquist L. & Springel V., 2003, MNRAS, 34, 1253
 Hughes D. H., et al., 1998, Nature, 394, 241
 Kauffmann G. & Haehnelt M., 2000, MNRAS, 311, 576
 Kauffmann G., et al., 2003, MNRAS, 346, 1055
 Kormendy J., Richstone D., 1995, ARA&A, 33, 581
 Lilly S. J., Le Fevre O., Hammer F., Crampton D., 1996, ApJ, 460, L1
 Madau P., Ferguson H. C., Dickinson M. E., Giavalisco M., Steidel C. C., Fruchter A., 1996, MNRAS, 283, 1388
 Madau P., Pozzetti L., Dickinson M. 1998, ApJ, 498, 106
 Magorrian, J. et al., 1998, AJ, 115, 2285
 Marconi A., Hunt L. K., 2003, ApJL, 589, L21
 Marconi A., Risaliti G., Gilli R., Hunt L. K., Maiolino R. & Salvati M., 2004, MNRAS, in press. astro-ph/0311619 (M04)
 McLure M. J. & Dunlop J. S., 2002, MNRAS, 331, 795
 Menci N., Cavaliere A., Fontana A., Giallongo E., Poli F., Vittorini V., 2003, ApJL, 587, L63
 Merloni A., 2004, MNRAS in press. astro-ph/0402495
 Merritt, D. & Ferrarese, L., 2001, MNRAS, 320, L30
 Miyaji T., Hasinger G., Schmidt M., 2000, A&A, 353, 25
 Monaco P., Salucci P. & Danese L., 2000, MNRAS, 311, 279
 Pascalelle S. M., Lanzetta K. M., Fernandez-Soto A., 1998, ApJ, 508, L1
 Pascual S., Gallego J., Aragón-Salamanca A., Zamorano J., 2001, A&A, 379, 789
 Richstone D., et al., 1998, Nature, 395, 14
 Rudnick G., et al., 2003, ApJ, 599, 847
 Salucci P., Persic M., 1999, MNRAS, 309, 923
 Sawicki M. J., Lin H., Yee H. K. C., 1997, AJ, 113, 1
 Schechter P. L., Dressler A., 1987, AJ, 94, 563
 Serjeant S., Gruppioni C., Oliver S., 2002, MNRAS, 330, 621
 Shankar F., Salucci P., Granato G. L., De Zotti G., Danese L., 2004, MNRAS, submitted. astro-ph/0405585
 Shields G. A., Gebhardt K., Salviander S., Wills B. J., Xie B., Brotherton M. S., Yuan J., Dietrich M., 2003, ApJ, 583, 124
 Soltan A., 1982, MNRAS, 200, 115
 Spergel D., et al., 2003, ApJS, 148, 175
 Steidel C. C., Adelberger K. L., Giavalisco M., Dickinson M., Pettini M., 1999, ApJ, 519, 1

Sullivan M., Treyer M. A., Ellis R. S., Bridges T. J., Milliard B., Donas J.,
2000, MNRAS, 312, 442
Tremaine S., et al., 2002, ApJ, 574, 554
Tresse L. & Maddox S. J., 1998, ApJ, 495, 691
Treyer M. A., Ellis R. S., Millard B., Donas J., Bridges T. J., 1998, MNRAS,
300, 303
Ueda Y., Akiyama M., Ohita K. & Miyaji T., 2003, ApJ, 598, 886
van den Bosch F. C., 1998, ApJ, 507, 601
Vestergaard M., 2004, ApJ, in press. astro-ph/0309521
Vignali C., Brandt W. N. & Schneider D. P., 2003, AJ, 125, 433
Volonteri M., Haardt F. & Madau P., 2003, ApJ, 582, 559
Wyithe J. S. B. & Loeb A., 2003, ApJ, 595, 614
Yu Q. & Tremaine S., 2002, MNRAS, 335, 965 (YT03)

This paper has been typeset from a \TeX / \LaTeX file prepared by the author.